Morphological Component Analysis based Compressed Sensing Technique on dynamic MRI reconstruction

Lei Yin and Ivan Selesnick
Department of Electrical and Computer Engineering,
Tandon School of Engineering,
New York University
ly652@nyu.edu and selesi@nyu.edu

***Abstract*— Compressive sensing (CS) MRI have been developed to speed up data acquisition without significantly degrading image quality. This paper proposes a novel compressed sensing reconstruction method exploiting temporally complementary morphological characteristics. This method relies on some well-developed signal processing techniques: morphological component analysis (MCA) and sparse derivatives. It also relies on well-developed MRI reconstruction techniques: incoherent undersampling schemes and parallel imaging. Other MRI schemes were simulated to make comparsion with our MCA-based CS method. CS and parallel imaging has been merged together to highly increase acceleration rate. This work simulates this framework also. Performance of applying different temporal regularizations individually and hybrid signal models based on MCA with and without auxilary spatial regularization are all analyzed in this paper. Nonlinear conjugate gradient algorithm is applied to gain all signal components simultaneously.**

***Index Terms*— Compressed Sensing, Morphological Component Analysis, Sparse Derivatives, Parallel Imaging**

I. INTRODUCTION

Magnetic resonance imaging has a wide range of clinical applications due to its benefit of being noninvasive, causing no radiation side effects, and offering excellent structure of body organs. However, long data acquisition time leads to patient discomfort, motion artifacts in reconstruction images, and lower temporal resolution in dynamic MRI. To overcome above disadvantages, fast acquisition schemes and high-quality reconstruction methods from undersampled data have been developed. Fast acquisition schemes, such as fast gradient echo imaging, fast spin echo imaging, and echo planar imaging (EPI), were designed with optimized pulse to shorten the acquisition time. But it is limited by physical constraints like gradient amplitude and slew rate for safety consideration. High-quality reconstruction from undersampled data, such as compressed sensing and parallel imaging, further increase the acceleration factor.

Compressive sensing is a signal processing technique that recovers certain signals through optimization from far fewer measurements than traditional methods [8]. Parallel imaging refers to the k-space data acquisition scheme by multicoils. Due to the independence of coil sensitivities, the image reconstruction become less ill-conditioned. The combination of above two techniques substantially increases the acceleration rate in MRI [5].

Since compressed sensing MRI model and a corresponding algorithm were first proposed [13], many improved CS MRI applications have emerged. Dynamic MRI based on CS model has been shown to retain satisfactory image quality and achieve higher spatial and temporal resolution by [5] [6] [14]. Most of these CS-based dynamic MRI methods are based on modeling the pixel intensity changes by assuming intensity of each voxel along temporal direction admit sparse represenatation in some transform domain, such as temporal DFT, total variation, and wavelet transform [11] [18] [19].

However, as shown in Fig. 1, some voxel time-intensity curves are not well captured by a single sparsifying transform. Consider one pixel example $\mathbf{s}$ within the right ventricle region. Its second-order difference $\mathbf{D_2 s}$ and its Fourier coefficients $\mathbf{\Phi}_{\text{DFT}}\mathbf{s}$ are shown in Fig. 1(b) and 1(c) repectively. It is clear that coefficients in above two transforms are not sparse. If signal model $\mathbf{s} = \mathbf{x}_1 + \mathbf{x}_2 + \mathbf{n}$ and corresponding decomposition method (1) are used to separate $\mathbf{s}$ into $\mathbf{x}_1$ and $\mathbf{x}_2$, in Fig. 2(a) and 2(c), then $\mathbf{\Phi}_{\text{DFT}}\mathbf{x}_1$ and $\mathbf{D}_2\mathbf{x}_2$ become much sparser.

$$\underset{\mathbf{x}_1,\mathbf{x}_2}{\operatorname{argmin}} \frac{1}{2}\|\mathbf{s}-\mathbf{x}_1-\mathbf{x}_2\|_2^2+\lambda_1\|\mathbf{\Phi}_{DFT}\mathbf{x}_1\|_1+\lambda_2\|\mathbf{D}_2\mathbf{x}_2\|_1 \quad (1)$$

In this paper, we propose the decomposition of intensity of each voxel along temporal direction into components based on some sparsifying transforms, such as sparse derivatives [1] and DFT. The proposed method is designed to preserve different morphological aspects of pixel intensity changes, which cannot be well modeled by just a single sparsifying transform.

The idea of decomposition-based MRI reconstruction were presented earlier in [2] [4]. In [2] the goal is to solve loss of low-contrast image features with increasing acceleration factors, and it is proposed that spatially piecewise smooth parts and residuals be separately coded by total variation and wavelets. The separation of low-rank and sparse components in dynamic MRI using principal component analysis and sparse signal representations is developed in [4]. Improved reconstruction accuracy were consistently obtained in different kinds of dynamic dataset by applying low-rank and sparse decomposition model.

The following sections describe our proposed method and compare it with some other state-of-the-art reconstruction

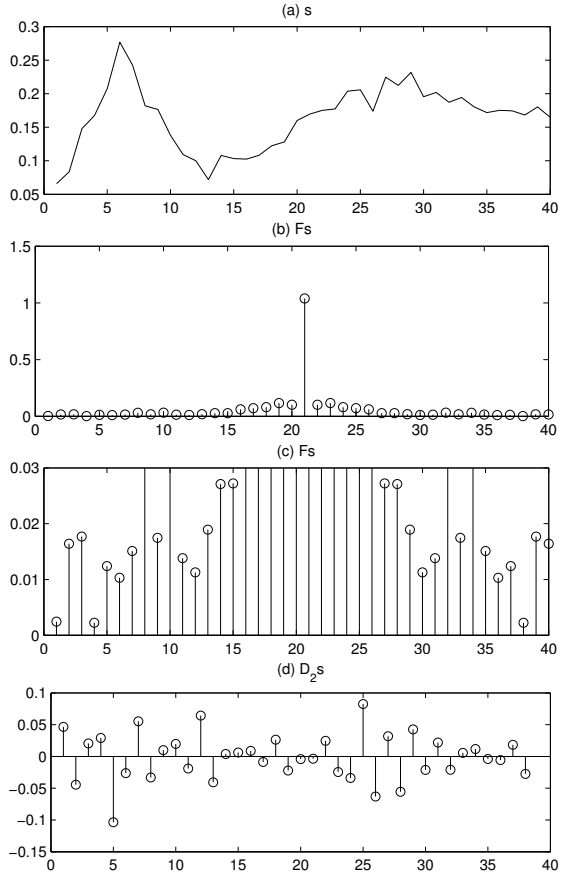

Fig. 1. (a) Time-intensity curve of one pixel example at index of $(56, 46)$. (b) The absolute value of Fourier coefficients of $\mathbf{s}$. (c) Show $\mathbf{Fs}$ between 0 and 0.03. (d) The second-order difference of $\mathbf{s}$.

schemes. As mentioned before, parallel imaging technique combined with other schemes have been proven to achieve good quality reconstruction even if high accelerated factor ($R = 8$) is chosen. Our MCA-based CS method is designed for both single channel and multichannel imaging. Section II discusses the proposed method in detail. The dataset and other state-of-the-art methods will be briefly described in Section III. Experimental simulation with $R = 8$ for both single channel and multichannel imaging are shown and analyzed in section III. Section IV makes a conclusion of the proposed MCA-based method, and discusses future work.

II. METHOD

Even though data acquisition by parallel coils is widely used in practical, some reconstruction techniques, such as k-t SLR [3], and DLTG [7], are designed for signal channel imaging. Data reconstruction assuming a single coil setup is involved when comparing with them. The subsection A describes the corresponding single channel signal model. The more practical signal model for multichannel is described in subsection B.

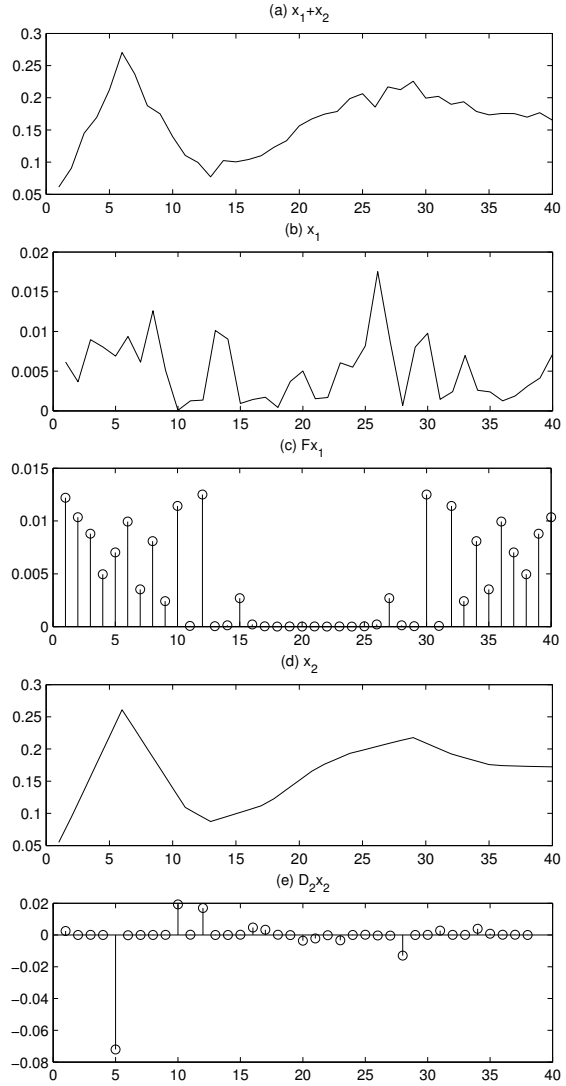

Fig. 2. (a) Estimated time-intensity curve of $\hat{\mathbf{s}} = \mathbf{x}_1 + \mathbf{x}_2$, and RMSE between $\mathbf{s}$ and $\hat{\mathbf{s}}$ is 0.004. (b) The DFT component $\mathbf{x}_1$. (c) The absolute value of Fourier coefficients of component $\mathbf{x}_1$. (d) The piecewise linear component $\mathbf{x}_2$. (e) The second-order difference of $\mathbf{x}_2$

A. Signal model for single channel dynamic MRI

Single channel acquired k-space data $\mathbf{y}_s$ can be formulated as

$$\mathbf{y}_s = \mathbf{M}\begin{bmatrix}\mathbf{F} & \dots & \mathbf{F}\end{bmatrix}\begin{bmatrix}\mathbf{m}_1 \\ \vdots \\ \mathbf{m}_n\end{bmatrix} + \mathbf{w} = \mathbf{H}_s\mathbf{m} + \mathbf{w} \qquad (2)$$

where $\mathbf{M}$ refers to the pseudorandom undersampling patterns shown in Fig. 3, $\mathbf{F}$ is Fourier transform in spatial domain for all time frames, $\mathbf{m} = \begin{bmatrix}\mathbf{m}_1 & \dots & \mathbf{m}_n\end{bmatrix}^H$ denote the concatenated image components, and $\mathbf{w}$ is additive Gaussian noise. The summation of n signal components $\sum_{i=1}^{n}\mathbf{m}_i$, is the desired image series.

B. Signal model for multichannel dynamic MRI

Parallel imaging has been applied in MRI to exploit data redundancy, especially when the number of receive

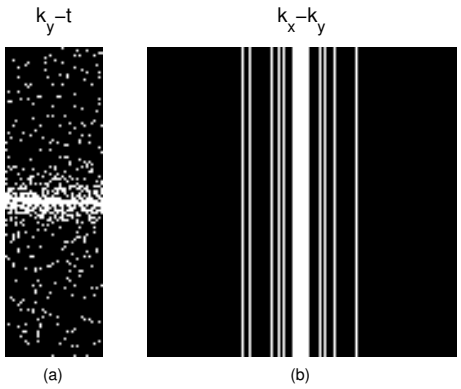

Fig. 3. The undersampling pattern used to increase spatial and temporal incoherence by randomly omitting phase-encoding lines with subsampling factor $R = 8$. (a) Indicates the k_y-t pseudorandom undersampling pattern, while (b) is k_x-k_y undersampling pattern at first time frame.

coils exceeds the acceleration factor R [12]. MRI applications combining compressed sensing and parallel imaging to further improve image quality has been addressed by several authors [5] [18] [19], via formulating parallel imaging technique into data fidelity term. The multi-channel k-space data $\mathbf{y}_m$ has been formulated as

$$\mathbf{y}_m = \mathbf{M}\begin{bmatrix}\mathbf{F} & \dots & \mathbf{F}\end{bmatrix}\mathbf{C}\mathbf{m} + \mathbf{w} = \mathbf{H}_m\mathbf{m} + \mathbf{w} \quad (3)$$

where $\mathbf{M}$, $\mathbf{F}$, $\mathbf{m}$ and $\mathbf{w}$ are defined exactly as above in single-channel case, $\mathbf{C}$ are formed by sorted coil sensitivity matrics $\mathbf{C}_i, i = 1, \dots, N_c$ as

$$\mathbf{C} = \begin{bmatrix}\mathbf{C}_1 \dots \mathbf{C}_1 \\ \vdots \dots \vdots \\ \mathbf{C}_{N_c} \dots \mathbf{C}_{N_c}\end{bmatrix}_{N_c \times n.} \quad (4)$$

C. Objective Function

Decomposition-based CS reconstruction assumes that intensity of each voxel as a function of time can be decomposed into several components whose represenatation in some certain transform domain are sparse. Aiming to achieve above signal model, the corresponding objective function is given by

$$\mathbf{m} = \underset{\mathbf{m}}{\operatorname{argmin}} \frac{1}{2}\|\mathbf{y} - \mathbf{H}_{s,m}\mathbf{m}\|_2^2 + \sum_{i=1}^{N} \lambda_i \Phi(\Psi_i \mathbf{m}_i) \quad (5)$$

where Ψ_i is the temporal sparsifying transform for component $\mathbf{m}_i$, Φ is a sparse-promoting function, such as l_1-norm, and λ_i is regularization weight to balance the contribution of component $\mathbf{m}_i$. Recently additional auxilary spatial penalty, such as spatial image gradient or spatial wavelet, has been proven to improve the reconstruction performance. Here we utilize this idea in our work. The objective function can be extended into following form:

$$\begin{aligned}\mathbf{m} = \underset{\mathbf{m}}{\operatorname{argmin}} \frac{1}{2}\|\mathbf{y} - \mathbf{H}_{s,m}\mathbf{m}\|_2^2 + \sum_{i=1}^{N} \lambda_i \Phi(\Psi_i \mathbf{m}_i) \\ + \alpha\Phi(\Psi_s[\mathbf{I}, \dots, \mathbf{I}]\mathbf{m})\end{aligned} \quad (6)$$

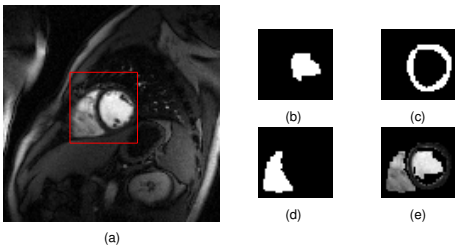

Fig. 4. (a) Ground true image reconstructed by Fourier transform of the fully sampled data. (b), (c) and (d) refer to the region of interest masks for left ventricle, myocardial wall and right ventricle respectively. (e) Indicates the whole heart.

where Ψ_s is the spatial image gradient transform, and its corresponding weight α can set equal to a small value to avoid oversoomthing or blurring in the image.

D. Solved by Nonlinear Conjugate Gradient (NCG)

Nonlinear conjugate gradient algorithm with backtracking line search has been provided by [13] to solve unconstrained problem. Within our formulated problem, there are n vector variables. In order to utilize NCG algorithm, we concatenate all signal components $\mathbf{m}_i$ together to create larger vector variable $\mathbf{m} = \begin{bmatrix}\mathbf{m}_1 \dots \mathbf{m}_n\end{bmatrix}^T$, and update $\mathbf{m}$ in each iteration. Therefore, all variables in the objective function can be obtained simultaneously. After all the signal components being obtained, summation all of them, $\sum_{i=i}^{n} \hat{\mathbf{m}}_i$, leads to the desired estimated result $\hat{\mathbf{m}}$.

An alternative algorithm for MCA-based objective function is proximal gradient algorithm (PG), described by [15] [16] [17]. MCA-based objective function without auxilary spatial regularization can simply utilize PG and its property of seperable sum by [16]. Compared with NCG, PG is designed for non-differentiable objective function, and is not necessary to smooth non-differentiable points.

E. Performance Measurements

To evaluate the quality of reconstructed images quantitatively, one measurement, called normalized root mean square error (NRMSE), is defined as

$$\text{NRMSE} = \sqrt{\frac{\sum_{i=1}^{n} |\mathbf{m}_{\text{acc}}(i) - \mathbf{m}_{\text{full}}(i)|^2}{\sum_{i=1}^{n} |\mathbf{m}_{\text{full}}(i)|^2}} \quad (7)$$

where $\mathbf{m}_{\text{acc}}$ refers to reconstructed image series by undersampled k-space data; $\mathbf{m}_{\text{full}}$ denotes reconstructed image series by fully-sampled k-space data; n is number of voxels in the region of interest times the number of time frames. In our work, three region of interests (ROIs): left ventricle (LV), myocardial wall (MW), and right ventricle (RV) are defined in Fig. 4 from 4(b) to 4(d).

Additionally, the temporal signal over left ventricle $\mathbf{s}_{lv}$ and myocardial wall $\mathbf{s}_{mw}$ contains important perfusion information. Thus, root mean square error (RMSE) between estimated $\hat{\mathbf{s}}$ and ground truth $\mathbf{s}$ can also quantitatively demon-

strates the performance of reconstruction methods.

$$\text{RMSE} = \sqrt{\frac{\sum_{i=1}^{n_t} |\hat{\mathbf{s}}(i) - \mathbf{s}(i)|^2}{n_t}} \quad (8)$$

III. EXPERIMENTAL RESULT

A. Dataset

Our MCA-based CS reconstruction are designed for both single channel and multichannel dynamic MRI dataset. In order to validate our proposed method, we applied it to a 12-channel first-pass cardiac perfusion dataset with imaging matrix of 128×128. This dataset is the same one used in parallel CS MRI [11]. The imaging parameters are exactly same as those described in [11]. The relevant imaging parameters include: FOV $= 320 \times 320$ mm, slice thickness $= 8$ mm, flip angle $= 10°$, TE/TR $= 1.2/2.4$ ms, BW $= 1000$ Hz/pixel, saturation-recovery time delay (TD) $= 10$ ms, repetitions $= 40$, spatial resolution $= 3.2$ mm $\times$ 3.2 mm, and temporal resolution $= 307$ ms. The ground truth for multichannel simulation is generated from fully sampled k-space data through least square combination [10], due to the availablity of coil sensitivity matrix. Other multi-channel techniques, such as low-rank and sparsity (L&S) [4] and k-t Sparse Sense [5], are also simulated in this paper to compare with our MCA-based CS scheme. To compare the proposed method with state-of-the-art methods designed for single channel imaging, such as k-t FOCUSS [6], k-t SLR [3], and DLTG [7], the ground truth for single-channel simulation is generated by normalizing that for multichannel. The corresponding single channel k-sapce is the Fourier coefficients of normalized ground truth.

B. Compared Methods

k-t FOCUSS, a general CS framework for dynamic MRI [6], has been proven to achieve high acceleration factor R. Besides, low-rank approximation (LR) and dictionary learning (DL) techniques are emerging to exploit the redundancies of MRI. k-t SLR and DLTG are two individual examples of LR and DL techniques for single channel imaging, and would be simulated and analyzed along with our methods (whose objective functions are shown in Table I). For MCA 1, we expect that tTV component $\mathbf{m}_2$ captures the intensity enhancement due to uptake of an injected MR contrast agent into myocardium. The remain frequency components can be captured by $\mathbf{m}_1$. Compared with MCA 1, MCA 2 only adds an auxilary spatial penalty with small weighted to improve the reconstruction performance. Reconstruction and their corresponding bar plots of NRMSE based on single channel imaging are shown in Fig. 5 and Fig. 6, respectively.

L&S and k-t Sparse Sense are two state-of-the-art schemes for multichannel reconstruction. Their simulation are also demonstrated along with that of multichannel MCA-based CS (whose objective functions are shown in Table II) in Fig. 7 and Fig. 8. Since parallel imaging technique is combined with MCA-based CS, problem itself becomes less ill-conditioned. Utilizing more signal components to model more detailed temporally complementary morphological characteristics of time-intensity curve becomes possible. For MCA 3, we also expect that tTV component $\mathbf{m}_2$ captures the intensity enhancement. In addition, we expect that tPL component $\mathbf{m}_3$ can mainly represent voxel time-intensity curves with slope discontinuity. The remain frequency components can be compensated by $\mathbf{m}_1$. Compared with MCA 3, MCA 4 only adds an auxilary spatial penalty.

TABLE I
MCA-BASED CS MODEL FOR SINGLE CHANNEL IMAGING

penalty	Objective Function
temporal TV & temporal DFT (MCA 1)	$\arg\min_{\mathbf{m}} \|\mathbf{y} - \mathbf{H}_s\mathbf{m}\|_2^2 + \lambda_{\text{tDFT}}\|\mathbf{\Psi}_{\text{tDFT}}\mathbf{m}_1\|_1 + \lambda_{\text{tv}}\|\mathbf{D}_1\mathbf{m}_2\|_1$
temporal TV & temporal DFT & spatial image gradient (MCA 2)	$\arg\min_{\mathbf{m}} \|\mathbf{y} - \mathbf{H}_s\mathbf{m}\|_2^2 + \lambda_{\text{tDFT}}\|\mathbf{\Psi}_{\text{tDFT}}\mathbf{m}_1\|_1 + \lambda_{\text{tv}}\|\mathbf{D}_1\mathbf{m}_2\|_1 + \alpha\|\mathbf{\Psi}_s[\mathbf{I},\mathbf{I}]\mathbf{m}\|_1$

TABLE II
MCA-BASED CS MODEL FOR MULTICHANNEL IMAGING

penalty	Objective Function
temporal TV & temporal PL & temporal DFT (MCA 3)	$\arg\min_{\mathbf{m}} \|\mathbf{y} - \mathbf{H}_m\mathbf{m}\|_2^2 + \lambda_{\text{tDFT}}\|\mathbf{\Psi}_{\text{tDFT}}\mathbf{m}_1\|_1 + \lambda_{\text{tv}}\|\mathbf{D}_1\mathbf{m}_2\|_1 + +\lambda_{\text{pl}}\|\mathbf{D}_2\mathbf{m}_3\|_1$
temporal TV & temporal PL & temporal DFT & spatial image gradient (MCA 4)	$\arg\min_{\mathbf{m}} \|\mathbf{y} - \mathbf{H}_m\mathbf{m}\|_2^2 + \lambda_{\text{tDFT}}\|\mathbf{\Psi}_{\text{DFT}}\mathbf{m}_1\|_1 + \lambda_{\text{tv}}\|\mathbf{D}_1\mathbf{m}_2\|_1 + \lambda_{\text{pl}}\|\mathbf{D}_2\mathbf{m}_3\|_1 + \alpha\|\mathbf{\Psi}_s[\mathbf{I},\mathbf{I},\mathbf{I}]\mathbf{m}\|_1$

C. Result Analysis

1) Single channel imaging: For perfusion dataset, temporal total variation (tTV) is a good model for sudden intensity changes along temporal direction, but introduces the staircase artifact in x-t and y-t slices (shown in row (b) and (c) of Fig. 5).

k-t FOCUSS [6], exploiting sparsity in y-f domain, can overcome above disadvantage and achieve good NRMSE, but requires a fully sampled frame as reference images. The actual acceleration factor R by k-t FOCUSS will be lower than other techniques. Thus, k-t FOCUSS sacrifices imaging speed a little for good reconstruction. Additionally, completion of stress perfusion was measured as the time to reach peak myocardial signal enhancement [9]. Second column row (e) of Fig. 5 demonstrates that averged temporal signal of MW reaches its peak 3 time frames earlier than the ground truth.

DLTG achieves good NRMSE in LV and RV areas, but not good in MW area. Result of (MCA 1) is comparable to k-t SLR at NRMSE of MW and whole heart when tTV and temporal DFT (tDFT) components together contribute the final reconstruction. Staircase artifacts have been reduced by adding tDFT component. (MCA 2) demonstrates that if auxilary spatial gradient penalty is applied, the reconstruction has been improved in both NRMSE of all ROIs and RMSE

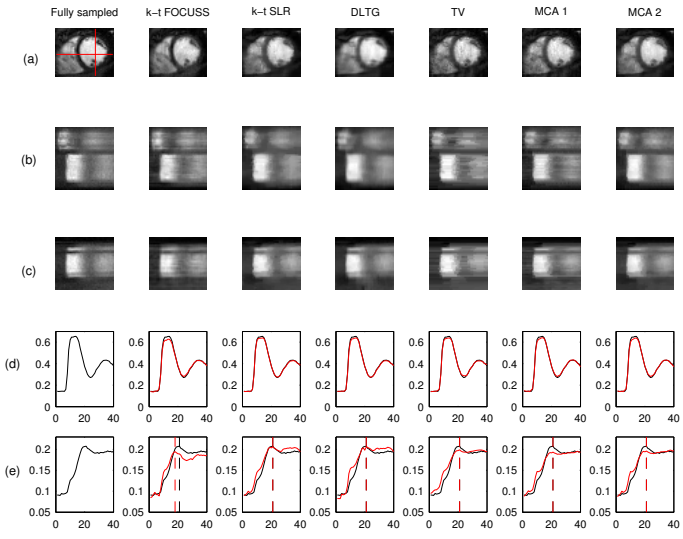

Fig. 5. Single-channel technique comparisions: The first column demonstrates the ground true result. Column 2 to 7 demonstrate the reconstruction by k-t FOCUSS technique, k-t SLR scheme, DLTG method, temporal total variation, our MCA based temporal technique and MCA based spatial-temporal technique, respectively. Row (a) shows the image frame at LV peak signal intensity. Rows (b) and (c) respectively show the x-t column time series and y-t row time series. Rows (d) and (e) demonstrate averaged temporal signal over left ventricle and myocardial wall respectively.

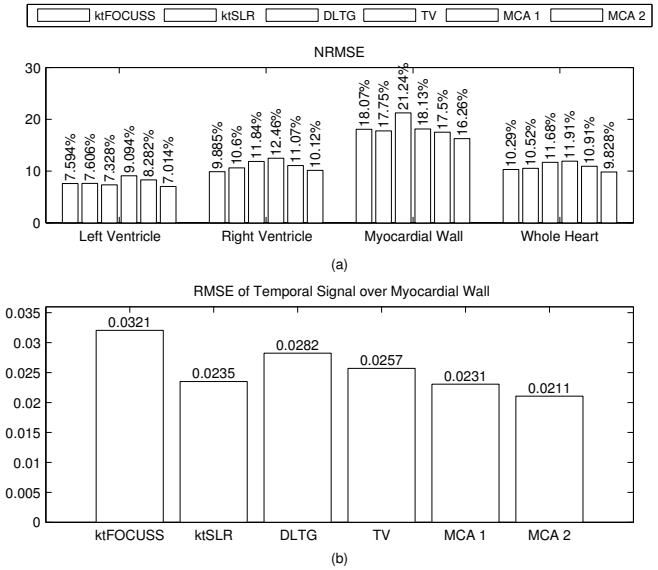

Fig. 6. (a) Indicates bar plot of NRMSE between each single-channel technique reconstruction with its ground truth over left ventricle (LV), myocardial wall (MW) and right ventricle (RV) respectively. (b) Indicates the RMSE of temporal myocardial wall signal for each single-channel techniques.

of temporal MW signal. Thus, more accurate reconstruction are achieved by (MCA 2).

2) Multichannel imaging: Parallel imaging can be combined with low rank approximation or CS methods. L&S and k-t Sparse Sense are two examples respectively. Except tTV, temporal second-order difference has been present in column five of Fig. 7. Sparse second-order difference coefficients promote piecewise linear form signal. Signal enhancement to peak usually takes about two time frames, and signal decay after high contrast takes more time frames. Thus, piecewise linear (PL) is a good optional signal model for dynamic MRI. Compared with tTV, tPL reduce the staircase artifact but smooth out the x-t and y-t slices. tTV achieves slightly better NRMSE than tPL does. However, RMSE of temporal MW signal shows that tPL reconstruction has a much better temporal signal to fit perfusion information.

(MCA 3) includes both tTV and tPL to balance the blockyness and smoothness in x-t and y-t slices. Thus, it suppresses the signal distortion that introduced by individual tTV or tPL. Besides, tDFT is also contained to compensate any frequency components. Fig. 8 demonstrates that (MCA 3) indeed take advantage of each of the components, and therefore achieves lower NRMSE of all ROIs and RMSE of temporal MV signal than individual tTV or tPL, L&S and k-t sparse sense. After auxilary spatial penalty being added, overall performance of like NRMSE and RMSE has been improved further. Result of (MCA 4) has the highest accuracy among that of all the demonstrated mathods in Fig. 7.

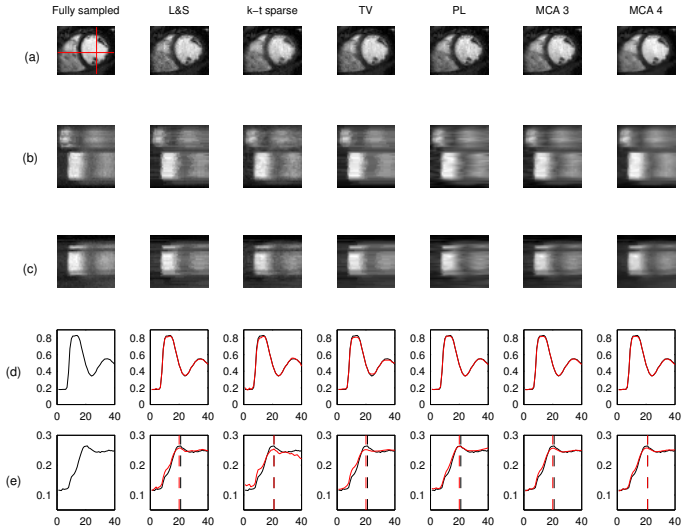

Fig. 7. Multichannel technique comparisions: The first column demonstrates the least square combination reconstruction, which can achieve optimal SNR. Column 2 to 7 demonstrate the reconstruction by low-rank and sparse technique, k-t sparse sense scheme, temporal total variation, temporal general total variation, our MCA based temporal technique and MCA based spatial-temporal technique, respectively. Rows (a) to (e) show the same information as Fig. 5.

IV. Conclusion and Future Work

We have presented a morphological component analysis based compressed sensing technique to highly accelerate MRI scans. The proposed method is shown to be able to gain more accurate results in comparsion with other MRI accelerating reconstruction scheme, especially combined with parallel imaging technique. It suppresses distortion and artifacts that occur when only a single signal component is

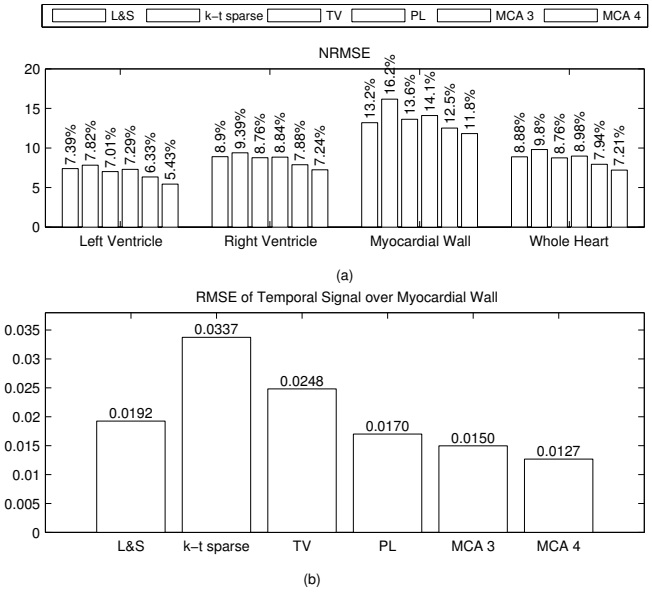

Fig. 8. (a) Indicates bar plot of NRMSE between each multi-channel technique reconstruction with its ground truth over LV, MW and RV respectively. (b) Indicates RMSE of temporal MW signal for each multi-channel schemes.

utilized.

For future work, we plan to extend the MCA-based CS reconstruction in radial trajectory k-space dataset. Radial trajectory is less sensitive to motion artifacts due to average of the center k-space coefficients. Less motion artifact results in stronger correlation between frames, which could achieve better performance in CS related reconstruction methods.

REFERENCES

[1] X. Ning, and I. Selesnick. ECG enhancement and QRS detection based on sparse derivatives. J. of Biomedical Signal Processing and Control, pages: 713-723, 2013.

[2] PS. Park and J. Park, "Compressed sensing MRI exploiting complementary dual decomposition", Med Image Anal, vol. 18, pp. 472-86, April 2014.

[3] S. G. Lingala, Y. Hu, E. DiBella and M. Jacob, "Accelerated dynamic mri exploiting sparsity and low-rank structure: kt SLR", IEEE Trans. Medical Imaging, vol. 30, no. 5, pp. 1042-1054, 2011.

[4] R. Otazo, E. Cands and D. K. Sodickson, "Low-rank plus sparse matrix decomposition for accelerated dynamic MRI with separation of background and dynamic components", Magn. Reson. Med., vol. 73, no. 3, pp. 1125-1136, Mar. 2015.

[5] R. Otazo, D. Kim, L. Axel and D. K. Sodickson, "Combination of compressed sensing and parallel imaging for highly accelerated first-pass cardiac perfusion MRI", Magn. Reson. Med., vol. 64, no. 3, pp. 767-776, Sep. 2010.

[6] H. Jung, K. Sung, K. S. Nayak, E. Y. Kim and J. C. Ye, "k-t FOCUSS: A general compressed sensing framework for high resolution dynamic mri", Magnetic Resonance in Medicine, vol. 61, no. 1, pp. 103-116, 2009.

[7] J. Caballero, A. Price, D. Rueckert and J. Hajnal, "Dictionary Learning and Time Sparsity for Dynamic MR Data Reconstruction", IEEE Transactions on Medical Imaging, vol. 33, pp. 979-994, Apr. 2014.

[8] E. Candes, M. Wakin, "An introduction to compressive sampling", IEEE Signal Processing Mag., vol. 25, no. 2, pp. 21-30, Mar. 2008.

[9] S. V. Raman, J. Dickerson, M. Jekic, E. Foster, M. Pennell, B. McCarthy, and O. Simonetti. Real-time cine and myocardial perfusion with treadmill exercise stress cardiovascular magnetic resonance in patients referred for stress SPECT. Journal of Cardiovascular Magnetic Resonance 12, no. 1 pp: 1-9, 2010

[10] P. B. Roemer, W. A. Edelstein, C. E. Hayes, S. P. Souza and O. M. Mueller, "The NMR phased array", Magn. Reson. Med., vol. 16, no. 2, pp. 192-225, 1990.

[11] C. Bilen, I. Selesnick, Y. Wang, R. Otazo, D. Kim, L. Axel, et al., "On compressed sensing in parallel MRI of cardiac perfusion using temporal wavelet and TV regularization", Proc. 2010 IEEE Int. Conf. Acoust. Speech Signal Process., pp. 630-633.

[12] R. Winkelmann, P. Brnert and O. Dssel, "Ghost artifact removal using a parallel imaging approach", Magn. Reson. Med., vol. 54, no. 4, pp. 1002-1009, Oct. 2005.

[13] M. Lustig, D. L. Donoho and J. M. Pauly, "Sparse MRI: The application of compressed sensing for rapid MR imaging", Magn. Reson. Med., vol. 58, no. 6, pp. 1182-1195, 2007.

[14] U. Gamper, P. Boesiger, and S. Kozerke. "Compressed sensing in dynamic MRI." Magnetic resonance in medicine 59(2): 365-373, 2008.

[15] P. L. Combettes and J.-C. Pesquet, "Proximal splitting methods in signal processing" in Fixed-Point Algorithms for Inverse Problems in Science and Engineering, 2010, Springer-Verlag.

[16] N. Parikh and S. Boyd, "Proximal algorithms", Found. Trends Optim., vol. 1, no. 3, pp. 123-231, 2013.

[17] J.-C. Pesquet and N. Pustelnik, "A parallel inertial proximal optimization method", Pac. J Optim., vol. 8, no. 2, pp. 273-305, Apr. 2012.

[18] L. Chaari, J.-C. Pesquet, A. Benazza-Benyahia and Ph. Ciuciu, "A wavelet-based regularized reconstruction algorithm for SENSE parallel MRI with applications to neuroimaging", Med. Image Anal., vol. 15, no. 2, pp. 185-201, Apr. 2011.

[19] L. Chaari, S. Mriaux, S. Badillo, J.-Ch. Pesquet and P. Ciuciu, "Multidimensional wavelet-based regularized reconstruction for parallel acquisition in neuroimaging", EURASIP Journal on Advances in Signal Processing, 2013.